Energy Saving Structural Health Monitoring Using Semi-Active Identification

Yushin Hara[1], Tianyi Tang[1], Keisuke Otsuka[1], Kanjuro Makihara[1]

[1] *Department of Aerospace Engineering, Tohoku University, Sendai, Miyagi, 980-8579, Japan*
yushin.hara.p1@alumni.tohoku.ac.jp

Abstract

This paper presents a novel approach to achieving system identification of a structure while minimizing energy consumption. The identified structural model can be used for structural health monitoring. In the aerospace environment, energy consumption is strictly regulated. To address this issue, we propose an energy-saving identification method that utilizes piezoelectric semi-active control as an input generation technique. This approach generates control force through electric switch activation, resulting in a smaller amount of energy consumption for input generation than conventional active control. We achieved semi-active input generation suitable for identification by incorporating a novel control strategy. The semi-active control has the disadvantage of limiting the free control of inputs. The identification performance may degrade if the properties of the semi-active input deviate from the desired ones. To address this issue, we also propose a data processing method that extracts a certain input with appropriate properties for identification from the acquired input. We validated the proposed method through numerical simulations and experiments. The results confirmed the feasibility of the semi-active identification method for structural health monitoring. Additionally, we found that the total energy consumption during the 20-second experiment was only 68 mJ to identify the 50 kg structure.

1. Introduction

Structural health monitoring (SHM) is critical in preventing severe operational issues that may arise from structural damage. Given the complexities involved in repairing aerospace structures during operation, monitoring techniques are essential (Tipaldi and Bruenjes, 2014). In this study, we discuss SHM using system identification. System identification provides an equivalent mathematical model of the target structure through input/output sequences. In a structural identification scenario, excitation forces and their responses correspond to I/O data. The structural damages are reflected in identified model variations (Deraemaeker, Reynders, De Roeck, and Kullaa, 2008). Achieving accurate identification is imperative to prevent any changes from being overlooked. Compared to SHM of on-ground structures, the SHM of aerospace structures faces constraints on energy consumption due to difficulties in securing electricity (Le et al., 2015). The objective of this study is to attain outstanding identification performance under energy constraints.

An energy-saving excitation force generator contributes to resolving concerns about energy consumption. Piezoelectric semi-active control is proposed as an energy-saving input generation method in the research field of vibration control (Richard, Guyomar, Audigier, and Ching, 1999). Unlike conventional piezoelectric active control that uses a signal amplifier and a function generator connected to a piezoelectric transducer, semi-active control does not require them. This method connects an electric circuit and an electric switch to the piezoelectric transducer as an input generator. Input is generated by actively controlling the connection and disconnection between the piezoelectric transducer and the additional circuit and passively inducing electrical resonance oscillation of electric charge, which drastically changes the polarity of an electric charge flowing into the transducer. As the switch control consumes little electricity, semi-active input generation is energy-saving.

However, piezoelectric semi-active control has two issues when adopted for identification (Hara, Otsuka, and Makihara, 2023a). First, it lacks a control strategy for the switch element because the piezoelectric semi-active control is proposed for vibration suppression rather than identification. Second, the semi-active input generation does not permit free control of inputs, which may result in degraded identification performance if the semi-active

input deviates from the ideal trajectory. We propose an input generation strategy and a post-data-processing method that make the semi-active input an ideal trajectory for system identification as much as possible.

This paper validates the accuracy of the semi-active identification method using the proposed strategy and data processing method. We confirm the proposed method achieves accurate identification while consuming only 65 μJ. The target structure in this study is a 2-degree-of-freedom structure.

2. Problem setting

2.1. Modeling

Fig. 1 shows an entire model. This study does not consider the nonlinearities of these components. The piezoelectric transducer is assumed to be deformed and polarized in one direction. The constitutive equations of the piezoelectric transducer (Hara, Tang, Otsuka, and Makihara, 2022) are described as

$$f_\mathrm{p} = k_\mathrm{p}\delta_\mathrm{p} - b_\mathrm{p}Q_\mathrm{p}, \tag{1}$$

$$v_\mathrm{p} = -b_\mathrm{p}\delta_\mathrm{p} + C_\mathrm{p}^{-1}Q_\mathrm{p}, \tag{2}$$

where f_p, v_p, δ_p, and Q_p denote the tensile force, voltage, deformation, and inflow charge of the piezoelectric transducer, respectively. The k_p, C_p, and b_p denote the constant-charge stiffness, constant-strain capacitance, and piezoelectric coefficient of the piezoelectric transducer, respectively. The subscript p indicates a value related to the piezoelectric transducer.

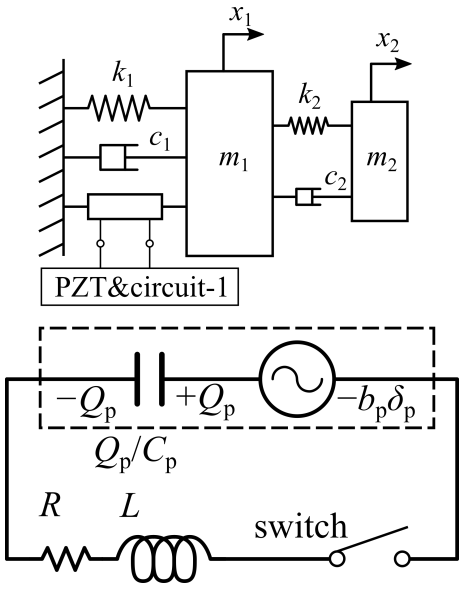

Figure 1. 2-DOF structure with 1-piece piezoelectric transducers and circuits.

The state space representation of the equation of motion of the 2-DOF structure in the modal coordinate is

$$\dot{\mathbf{z}}_\mathrm{m} = \mathbf{A}_\mathrm{m}\mathbf{z}_\mathrm{m} + \mathbf{B}_\mathrm{m}\mathbf{q}_\mathrm{p} + \mathbf{E}\mathbf{d}, \tag{3}$$

where

$$\begin{aligned} &\mathbf{z}_\mathrm{m} \equiv \begin{bmatrix}\boldsymbol{\eta}^T & \dot{\boldsymbol{\eta}}^T\end{bmatrix}^T, \quad \mathbf{A}_\mathrm{m} \equiv \begin{bmatrix}\mathbf{0} & \mathbf{I} \\ -\boldsymbol{\Omega}_\mathrm{m}^2 & -2\boldsymbol{\Xi}_\mathrm{m}\boldsymbol{\Omega}_\mathrm{m}\end{bmatrix}, \\ &\mathbf{B}_\mathrm{m} \equiv \begin{bmatrix}\mathbf{0} \\ \boldsymbol{\Phi}^T\boldsymbol{\Theta}\mathbf{B}_\mathrm{p}\end{bmatrix}, \quad \text{and} \quad \mathbf{E} \equiv \begin{bmatrix}\mathbf{0} \\ \boldsymbol{\Phi}^T\end{bmatrix}. \end{aligned} \tag{4}$$

The $\boldsymbol{\eta}$, $\mathbf{q}_\mathrm{p}$, and $\mathbf{d}$ denote the modal displacement, piezoelectric charge, and displacement vectors, respectively. The $\boldsymbol{\Xi}_\mathrm{m}$, $\boldsymbol{\Omega}_\mathrm{m}$, and $\mathbf{B}_\mathrm{p}$ denote the modal damping ratio, modal angular frequency, input coefficient matrices:

$$\begin{aligned} &\boldsymbol{\Xi}_\mathrm{m} \equiv \mathrm{diag}\begin{bmatrix}\xi_1 & \cdots & \xi_q\end{bmatrix}, \quad \boldsymbol{\Omega}_\mathrm{m} \equiv \mathrm{diag}\begin{bmatrix}\omega_1 & \cdots & \omega_q\end{bmatrix}, \\ &\text{and} \quad \mathbf{B}_\mathrm{p} \equiv \mathrm{diag}\begin{bmatrix}b_{\mathrm{p},1} & \cdots & b_{\mathrm{p,m}}\end{bmatrix}. \end{aligned} \tag{5}$$

The $\boldsymbol{\Phi}$ is the transfer matrix between physical and normal mode coordinates. The $\boldsymbol{\Theta}$ is the position matrix indicating the mass on which the force acts:

$$\boldsymbol{\Theta} \equiv \begin{bmatrix} 1 & -1 & & 0 \\ & \ddots & \ddots & \\ 0 & & 1 & -1 \end{bmatrix}. \tag{6}$$

Finally, the circuit equation is derived. An inductor-resistor circuit and switch element connect to the piezoelectric transducer. Since the piezoelectric transducer model has the capacitance component (see Eq. 2), the entire circuit construction is the inductor-capacitor-resister (LCR) circuit having a deformation-dependent voltage source while the switch element is closing. There are two circuit equations depending on the switch states:

$$\dot{Q}_\mathrm{p} = 0 \quad \text{(when switch is open)}, \tag{7}$$

$$L\ddot{Q}_\mathrm{p} + R\dot{Q}_\mathrm{p} + C_\mathrm{p}^{-1}Q_\mathrm{p} = b_\mathrm{p}\delta_\mathrm{p} \quad \text{(when switch is closed)}, \tag{8}$$

where L and R denote the inductance and resistance in the additional circuit, respectively.

The switch element is typically in an open state. The duration in the closed state corresponds to the half-period of the LCR oscillation. The act of closing the switch element for the designated time period is referred to as "switching". During this process, the piezoelectric charge oscillates. Adjusting the additional inductance so that the electrical resonance frequency will be significantly higher than the frequencies of mechanical vibrations causes the deformation-dependent voltage to be regarded as a constant value. The piezoelectric charge before and after the

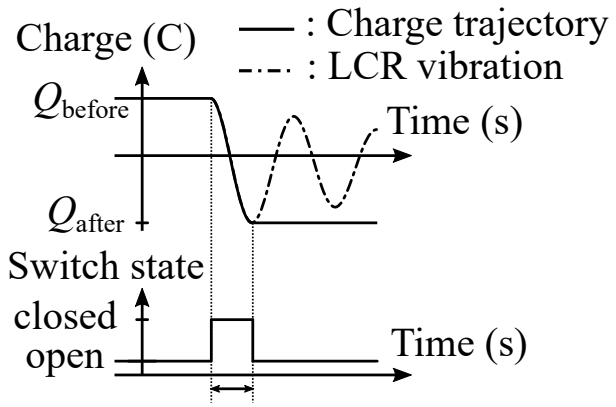

Figure 2. Enlarged time trajectory of semi-active input during switching.

single-switching activation can be expressed as:

$$Q_{\text{after}} \equiv Q_{\text{p}}\left(\frac{\pi}{\omega_{\text{e}}}\right) = -\gamma Q_{\text{before}} + \left(1+\gamma\right) b_{\text{p}} C_{\text{p}} \delta_{\text{switching}}, \quad (9)$$

where

$$\gamma \equiv \exp(-\xi_{\text{e}}\pi), \quad \omega_{\text{e}} \equiv \sqrt{\frac{1}{LC_{\text{p}}}}, \quad \text{and} \quad \xi_{\text{e}} \equiv \frac{R}{2}\sqrt{\frac{C_{\text{p}}}{L}}. \quad (10)$$

Here, Q_{before} and Q_{after} represent the piezoelectric charge before and after the switching, respectively. The $\delta_{\text{switching}}$ denotes the constant deformation value obtained at the start of the switching process. The piezoelectric charge oscillation results in a drastic change in the piezoelectric charge. Fig. 2 illustrates the time history of the piezoelectric charge. Moreover, the switching duration is very short, lasting only a few milliseconds. In this study, a photo-MOSFET, PS7205B-1A, was used as the switching element, which consumes 65 μJ during each switching action.

The amplitude of the piezoelectric charge after the switching depends on the magnitude of the deformation $\delta_{\text{switching}}$. The deformation depends on the mechanical vibration of the structure. The mechanical vibration is excited by the uncontrollable disturbance. The amplitude of the piezoelectric charge cannot be freely adjusted by the switching, whereas the polarity of the piezoelectric charge can be arbitrarily adjusted when the following inequality holds (Hara, Tang, Otsuka, and Makihara, 2023b):

$$Q_{\text{before}}\left(Q_{\text{before}} - \frac{b_{\text{p}} C_{\text{p}}\left(1+\gamma\right)}{\gamma}\right) < 0. \quad (11)$$

Table 1 summarizes the performance of the abilities of both conventional active and proposed semi-active input generation methods. The semi-active identification method must be performed in accordance with the shortcomings of the semi-active input generation method.

2.2. Maximum-Length Sequence

A maximum-length sequence (MLS) that is a pseudorandom periodic sequence has broadband frequency components. Because the MLS can excite broadband structural responses, the MLS has been widely used in conventional identification. This study used two-level MLS. The two-level MLS takes two sets of values representing two levels of the signal. The signal shape of the MLS is similar to the square wave having a constant amplitude and a non-constant period. The MLS generation uses the following discrete-time state-space equations

$$\mathbf{z}_{\text{MLS}}(i+1) = \mathbf{A}_{\text{MLS}}\mathbf{z}_{\text{MLS}}(i), \quad (12)$$

$$y_{01}(i) = \mathbf{C}_{\text{MLS}}\mathbf{z}_{\text{MLS}}(i), \quad (13)$$

where

$$\mathbf{z}_{\text{MLS}}(i) \equiv \begin{bmatrix} z_{\text{MLS},1}(i) & \cdots & z_{\text{MLS},n}(i) \end{bmatrix}^T,$$
$$\mathbf{A}_{\text{MLS}} \equiv \begin{bmatrix} a_1 & a_2 & \cdots & a_{n-1} & a_n \\ 1 & 0 & \cdots & 0 & 0 \\ 0 & 1 & \cdots & 0 & 0 \\ \vdots & & \ddots & & \vdots \\ 0 & 0 & 0 & 1 & 0 \end{bmatrix}, \quad (14)$$
$$\text{and} \quad \mathbf{C}_{\text{MLS}} \equiv \begin{bmatrix} 0 & 0 & \cdots & 0 & 1 \end{bmatrix}.$$

The feedback coefficients a_n determine the period of the MLS. When the appropriate coefficients are used, the period of the two-level MLS is $2^n - 1$. Notably, the operation of Eq. 12 is modulo-2 arithmetic. The two-level MLS composed of 0 and 1 maps to -1 and $+1$ to bring the average value of the MLS close to zero:

$$y_{-+}(i) = 2y_{01}(i) - 1. \quad (15)$$

In this paper, the 2-level MLS composed of the six feedback coefficients ($n = 6$) is applied. The definition of feedback coefficients are

$$\begin{bmatrix} a_1 & a_2 & \cdots & a_5 & a_6 \end{bmatrix} \equiv \begin{bmatrix} 1 & 0 & 0 & 0 & 0 & 1 \end{bmatrix}. \quad (16)$$

Figs. 3 and 4 show the time trajectory, power spectral density, and autocorrelation of the 2-level MLS generated using Eq. 12. The MLS is similar to the band-limited white noise because its power spectral density is flat.

3. Proposed Methods

3.1. Maximum-Length Sequence Switch Identification on Inductor

The semi-active identification method is inspired by the shape similarity between the MLS and semi-active input.

Table 1. Abilities of active and semi-active input generation

Method	Input amplitude control	Input polarity control	Energy consumption
Active	Possible	Possible	Large
Semi-active	Impossible	Possible while Eq.(11) is hold	Small

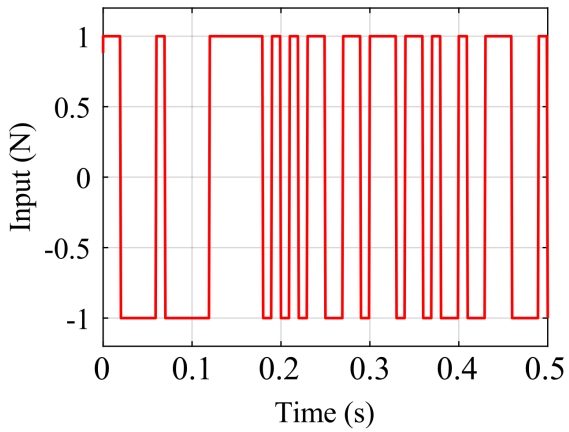

Figure 3. Time trajectory of MLS.

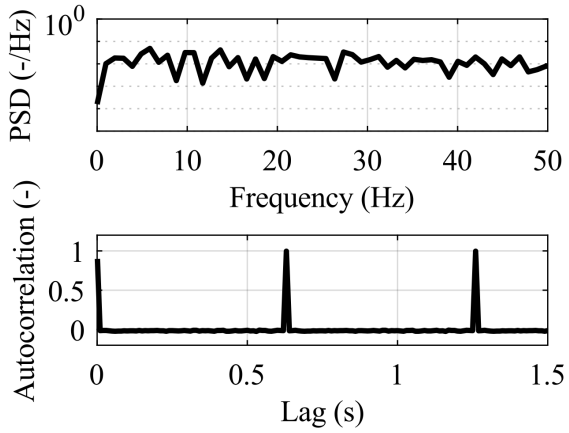

Figure 4. PSD and autocorrelation of MLS.

To generate semi-active input imitating the MLS, we introduce target signal Q_{t} as

$$Q_{\mathrm{t}}(i) = y_{-+}(i). \tag{17}$$

The semi-active input Q_{p} traces the target signal Q_{t} to perform the same identification performance as the conventional cases using the MLS directly. Eq. 9 indicates that the polarities of the semi-active input before and after switching are opposite. The following switching strategy is presented:

Strategy When $Q_{\mathrm{t}}(i-1)\cdot Q_{\mathrm{t}}(i) < 0$, the switch element is turned on during π/ω_{e}.

This strategy is referred to as a maximum-length sequence switch identification on inductor (MLSII).

3.2. Extraction of Appropriate Input Using Sign Similarity

The semi-active input, owing to its generation mechanism, cannot fully replicate the MLS. It is imperative to select time intervals that are most suitable for identification from the entire semi-active input sequence. The MLS is a pseudo-random periodic sequence, and the response of the structure is also periodic when the MLS is applied directly to the structure. A segment is a data region that is divided by the MLS period. Ideally, the identification results should not differ regardless of which segment is used. If the semi-active input adequately emulates the MLS, the semi-active input and its responses may also be periodic. We segment the semi-active input and response sequences based on the MLS period and select the segments that exhibit higher similarity for use in identification. The similarity in sign (polarity) is determined using the Hamming distance between the polarities of the MLS and the semi-active input.

1. The positive and negative semi-active input, Q_{p} is mapped to 1 and 0, respectively. The Q_{01} indicates the mapped input.
2. The acquired input/output sequences are divided into several segments. The length of one segment corresponds to the period of the MLS, T_{MLS}.
3. The Hamming distance of k-th segment is

$$d_{\mathrm{Hamming},k} \equiv \int_0^{T_{\mathrm{MLS}}} \delta\left(y_{01}(t), Q_{01,k}(t)\right) dt, \tag{18}$$

where

$$\delta\left(y_{01}(t), Q_{01,j,k}(t)\right) \equiv \begin{cases} 1 & y_{01}(t) \neq Q_{01,k}(t), \\ 0 & y_{01}(t) = Q_{01,k}(t). \end{cases} \tag{19}$$

4. The sign similarity of the k-th segment is calculated from the Hamming distance:

$$\mu_{\mathrm{sign},k} \equiv 1 - \frac{d_{\mathrm{Hamming},k}}{T_{\mathrm{MLS}}}. \tag{20}$$

5. The input/output sequences are rearranged using the obtained sign similarities in the order of segments with a high degree of similarity. The output data are also sorted in line with the input sorting.

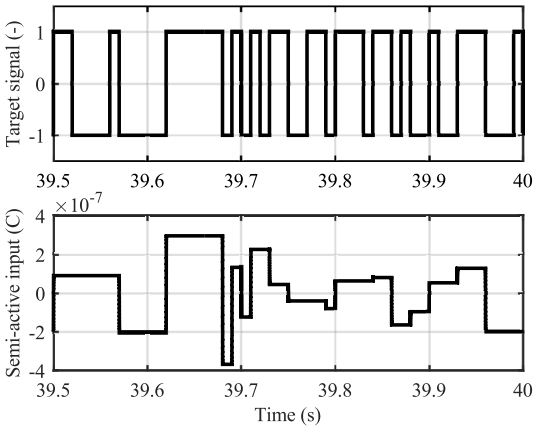

Figure 5. Enlarged time trajectories of semi-active input and target signal generated by MLSII strategy.

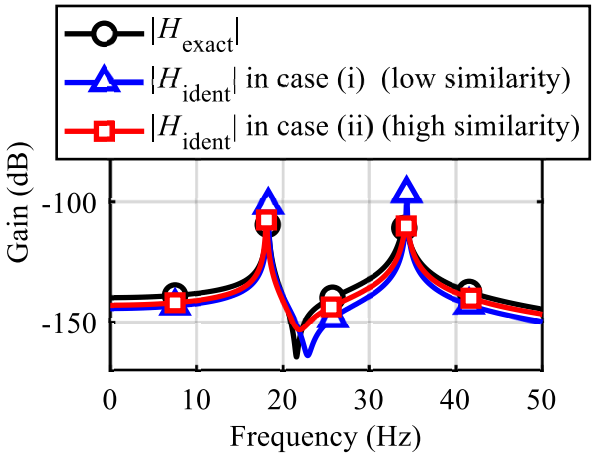

Figure 6. Numerical identification result using MLSII strategy and data extraction method.

4. Numerical Simulation

4.1. Simulation Setup

A simulation was conducted. The identification target was the 2-DOF structure, which was equipped with a single piezoelectric transducer and a single laser displacement sensor. A 10 Hz periodic disturbance was applied to the structure. To obtain a structure model, the multivariable output-error state space (MOESP) method (Verhaegen and Dewilde, 1992) was employed.

4.2. Generated Semi-Active Input

The time histories of the target signal and the semi-active input produced by the MLSII strategy are presented in an enlarged format in Fig. 5. The amplitudes of the target signal remained constant at −1 and 1. However, due to limitations in the semi-active input generation circuit, the amplitude of the semi-active input could not be controlled and thus, did not remain constant. Additionally, the polarities of the two signals often coincided but were not always synchronized due to the limitations of the piezoelectric semi-active control.

4.3. Identification Performance

The semi-active identification result illustrated in Fig. 6 utilized the data extraction method, which retrieved segments with high sign similarity. Seven segments exhibiting high sign similarity were extracted, while the sections with low sign similarities were utilized to derive the identification result for comparison. The segments with high sign similarities were employed in case (ii), while the segments with low sign similarities were employed in case (i). From this numerical simulation, two important aspects were confirmed. Firstly, the feasibility of system identification with a semi-active input was demonstrated. Additionally, it was confirmed that the identification result can be improved by preferentially utilizing the region where the polarities of the semi-active input and the MLS coincide, as demonstrated through the comparison of the two results.

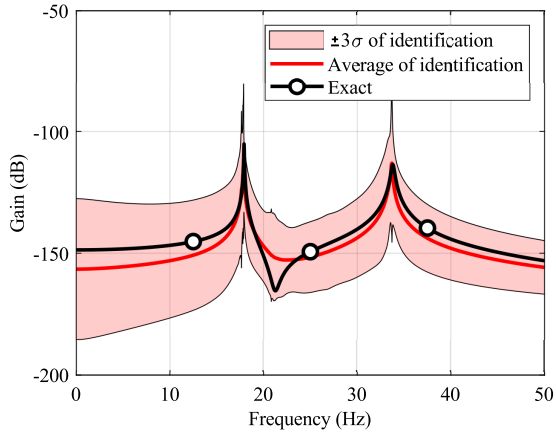

Figure 7. 190 experimental identification results of semi-active identification method using MLSII strategy.

5. EXPERIMENT

The performance of identification was assessed through experimentation, where the experimental conditions corresponded to the simulation. A 10 Hz disturbance was applied to the 2-DOF structure, and a total of 190 identification experiments were conducted. The means and variances of these experiments are illustrated in Fig. 7, where the translucent region represents a region three times the standard deviation (3σ) of the 190 identification trials. It is noteworthy that the exact model was included within the 190 trials, and the average of the identification results was found to be in close proximity to the

exact model. Therefore, the feasibility of the semi-active identification method using the MLSII strategy was confirmed, and the consumption of energy was a mere 68 mJ.

6. CONCLUSION

This study introduces a groundbreaking method for structural identification using a semi-active input generated from a piezoelectric transducer. The semi-active input possesses suitable properties for identification. A simple LCR circuit is employed to generate the semi-active input, which consumes very little energy, making the semi-active identification method accessible for in-situ structural identification and SHM.

A novel switching strategy is proposed, referred to as the MLSII strategy, which performs switching to match the polarity of the semi-active input to that of the MLS. The MLS is widely used in conventional identification. However, there may be mismatches of polarities resulting in the inability of the semi-active input to imitate the polarity of the MLS. To address this issue, a data calibration method is proposed, considering the sign similarity between the semi-active input and the MLS. The similarity is indicated by the Hamming distance, and segments with higher sign similarity are used for identification.

The performance of the semi-active identification method is evaluated through numerical simulation and experiment. It appropriately identified the 2-DOF structure model. This theory has the potential to identify a higher DOF than the 2-DOF model when the target structure satisfies the observability and controllability. The consumption energy of the semi-active input generation is smaller than that of the conventional active input generation, making the semi-active identification method both applicable and feasible.

ACKNOWLEDGMENT

This work was supported by the Grant-in-Aid for JSPS Fellows (KAKENHI) (grant numbers 22H01675 and 23H01366) from the Japan Society for the Promotion of Science.

REFERENCES

Deraemaeker, A., Reynders, E., De Roeck, G., Kullaa, J. (2008). Vibration-based structural health monitoring using output-only measurements under changing environment. *Mechanical Systems and Signal Processing*, *22*(1), 34–56. doi: 10.1016/j.ymssp.2007.07.004

Hara, Y., Otsuka, K., Makihara, K. (2023a). Low-energy-consumption structural identification with switching piezoelectric semi-active input. *Mechanical Systems and Signal Processing*, *187*, 109914. doi: 10.1016/j.ymssp.2022.109914

Hara, Y., Tang, T., Otsuka, K., Makihara, K. (2022). Self-sensing method for semi-active structural identification by removing piecewise bias from piezoelectric voltage. *Sensors and Actuators A: Physical*, *347*, 113907. doi: 10.1016/j.sna.2022.113907

Hara, Y., Tang, T., Otsuka, K., Makihara, K. (2023b). Strategy for performance improvement in piezoelectric semi-active structural system identification by excluding switching failures using pseudo-state feedback. *Mechanical Systems and Signal Processing*, *187*, 109906. doi: 10.1016/j.ymssp.2022.109906

Le, M. Q., Capsal, J. F., Lallart, M., Hebrard, Y., Van Der Ham, A., Reffe, N., ... Cottinet, P. J. (2015). Review on energy harvesting for structural health monitoring in aeronautical applications. *Progress in Aerospace Sciences*, *79*, 147–157. doi: 10.1016/j.paerosci.2015.10.001

Richard, C., Guyomar, D., Audigier, D., Ching, G. (1999). Semi-passive damping using continuous switching of a piezoelectric device. In *Smart structures and materials 1999: Passive damping and isolation.* doi: 10.1117/12.349773

Tipaldi, M., Bruenjes, B. (2014). Spacecraft health monitoring and management systems. In *2014 ieee metrology for aerospace (metroaerospace)* (pp. 68–72). doi: 10.1109/MetroAeroSpace.2014.6865896

Verhaegen, M., Dewilde, P. (1992). Subspace model identification Part 2. Analysis of the elementary output-error state-space model identification algorithm. *International Journal of Control*, *56*(5), 1211–1241. doi: 10.1080/00207179208934364

BIOGRAPHIES

Yushin Hara was born in Japan. He received his Ph.D. degree in 2023 from Tohoku University. He has been a researcher at Tsukuba University since 2023.

Tianyi Tang was born in China. He received his master degree in 2023 from Department of Aerospace Engineering, Tohoku University. He has been in a doctoral program at Tohoku University since 2023.

Keisuke Otsuka was born in Japan. He received his Ph.D. degree in 2020 from Tohoku University. He has been an associate professor at Tohoku University since 2023.

Kanjuro Makihara was born in Japan. He received his Ph.D. degree in 2004 from the University of Tokyo. He has been a professor at Tohoku University since 2019.